Statistical approach to nondiffractive hadron-hadron collisions: Multiplicity distributions and correlations in different rapidity intervals

Cai Xu,* Chao Wei-qin,† and Meng Ta-chung
Fachbereich Physik der FU Berlin, Berlin, Germany

Huang Chao-shang
Institute of Theoretical Physics, Academia Sinica, Beijing, China
(Received 6 August 1985)

It is shown that the recently observed pseudorapidity-interval dependence in multiplicity distributions and the existence of positive long-range correlations between the numbers of charged particles in different pseudorapidity intervals give further evidence for the statistical nature of nondiffractive hadron-hadron collision processes. Quantitative predictions are made for future experiments at higher bombarding energies. It is pointed out in particular that for every (sufficiently high total c.m.-system) energy $\sqrt{s}$, there exists a (pseudo)rapidity interval W in which the probability $P_W(n_W)$ to find n_W charged hadrons (in this given interval) satisfies $\langle n_W\rangle P_W(n_W)=4n_W/\langle n_W\rangle \times\exp(-2n_W/\langle n_W\rangle)$, where $\langle n_W\rangle$ is the average value of n_W.

I. INTRODUCTION

In a recent paper[1] the UA5 Collaboration published their investigation of multiplicity distributions in different pseudorapidity intervals (W) in $\bar{p}p$ reactions at center-of-mass-system (c.m.s.) energy $\sqrt{s}=540$ GeV. It is observed that the width of the multiplicity distributions, scaled to their means, increases as W is made smaller. In particular, the corresponding Kuba-Nielsen-Olesen (KNO) plot [that is, $\langle n_W\rangle P_W(n_W)=\psi_W(z_W)$ as a function of $z_W=n_W/\langle n_W\rangle$, where n_W is the charge multiplicity observed in the given pseudorapidity window W, $\langle n_W\rangle$ is its average value, and $P_W(n_W)$ is the probability to find n_W charged hadrons within the window W] changes its form in the following way. (i) The position of the maximum value $z_{W\,\max}$ moves to smaller values for smaller pseudorapidity windows. (ii) The curve of $\psi_W(z_W)$ at large-z values becomes more and more flat when the size of the windows decreased. That is, the relative number of large-fluctuation events increases for smaller pseudorapidity windows. Furthermore it is found that, for a given pseudorapidity interval ($W=0.4$, 1, and 2), the moments of the multiplicity distributions remain practically the same when the center of the interval is shifted from $\eta=0$ to other values, provided that it is not taken too far away from $\eta=0$.

The purpose of this paper is to show that the above-mentioned new experimental results[1] as well as the existence of positive long-range correlations between the numbers of charged particles in different pseudorapidity intervals[2,3] give further evidence for the statistical nature of high-energy nondiffractive hadron-hadron collisions.

II. THE MODEL

A model based on statistical methods was suggested[4] some time ago in order to understand the non-single-diffractive hadron-hadron collision data[5] at high energies. While the basic ideas and the main results remain unchanged, some of the details of the proposed semiclassical picture need to be modified. The underlying physical picture of this model is the following. In a typical (here we neglect the violent collision events which are rare; for further details see Ref. 4 and the papers cited there) high-energy nondiffractive hadron-hadron collision event the projectile P and the target T can be envisaged as spatially extended objects which go through each other and appear as leading particles. While going through and interacting with each other, the colliding objects P and T lose a considerable part of their energies and momenta. A part of this "lost energy" materializes—in general, into a number of clusters[6] which subsequently decay into hadrons. This part of energy—the materialization energy—is distributed in three distinct systems C^*, P^*, and T^* which are characterized by their locations in rapidity space. (Here C^* stands for the central rapidity region, and P^* and T^* stand for the projectile- and target-fragmentation regions, respectively.) In terms of the conventional quark-gluon picture,[7] in which hadrons are made out of valence quarks and gluons, and on the average about 35—50% of the momentum of a high-energy hadron is carried by its valence quarks and the rest by the gluons (and/or sea-quark pairs), the hadronic matter created in system C^* is due to the interaction between the gluons (and/or sea-quark pairs) in the projectile and their counterparts in the target. That is, the clusters in system C^* obtain their energies and momenta from *two* sources, namely, the gluon part (gluons and/or sea-quark pairs) of the projectile and that of the target. Similarly, the materialization energy in the system P^* (T^*) is also due to two energy-momentum sources, namely, the energy-momentum of the quark part and that of the gluon part of the projectile (target). That is to say, the quark-gluon picture implies that the number of such two-source systems in high-energy nondiffractive

hadron-hadron collision processes should be *three*. This point is illustrated in Fig. 1.

Each of the three excited systems (C^*,P^*,T^*) is assumed to have the following properties.

(i) The amount of energy contributed by each of the two sources to the materialization energy of the system is a *random* variable. After the materialization, the system *"forgets its history"* in the sense that the probability of forming such a system characterized by the total amount of materialization energy does not depend on the specific way of its formation. In particular, it "does not remember" how much of this materialization energy is due to one source, and how much of it is due to the other source. Another way of expressing the second part of this assumption is the following. In a system characterized by a given total amount of materialization energy, because of the above-mentioned randomness, the difference between the contributions of the two sources may have any one of the possible values in the corresponding energy range. Since there is no *a priori* reason why the occurrence of a particular value in this range should be more probable than others, it is assumed that any one of these values is equally likely to occur.

(ii) The amount of momentum contributed by each of the two sources to the net momentum of any one of the clusters of the system is also *random*. As a consequence, the rapidities of the clusters in the system may have any one of the possible values in the corresponding kinematical region. Since there is no *a priori* reason why any particular one of these values should be preferred, it is assumed that their occurrences are *equally probable*.

Because of the fact that the key features of the present model are characterized by notions such as randomness, memory loss and/or equal probability, and that very little knowledge on the quark-gluon dynamics such as QCD has been incorporated, a comparison between data and model will yield useful information on the following question: Are high-energy nondiffractive hadron-hadron collisions statistical processes?

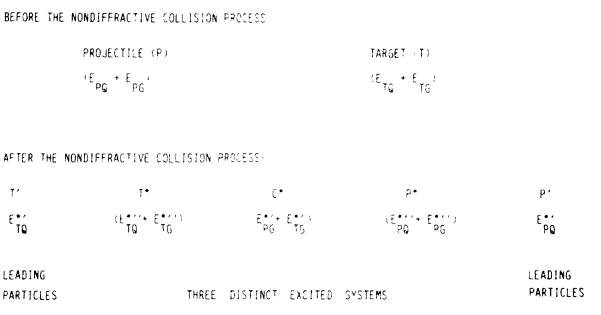

FIG. 1. Formation of the three excited hadronic systems C^*,P^*,T^* in high-energy nondiffractive hadron-hadron collisions. Here E_{PQ} stands for the energy of the quark part, and E_{PG} for that of the gluon part (gluons and/or sea-quark pairs) of the projectile P. $E^{*\prime}_{PQ}$ denotes the internal energy of the group of leading particles P'. This group has the same quantum numbers as those of the projectile P. $E^{*\prime}_{PG}$ and $E^{*\prime\prime}_{PG}$ are, respectively, the contributions to the materialization energy of the system C^* and that of P^* from the gluon-part of the projectile. $E^{*\prime\prime}_{PQ}$ is the contribution to the materialized energy of P^* from the quark part of the projectile. The symbols E_{TQ}, etc., have similar meanings. Note that all the quantities with asterisks are internal energies which are measured in the rest frames of the corresponding materialized objects. Note also that all these quantities are random variables.

First, we note that assumption (i) implies the following (see Appendix A). The materialization energy E_i^* of the system i $(i=C^*,P^*,T^*)$ is distributed in the following way (we omit the asterisks on the subscripts; that is, we write E_C^* instead of $E_{C^*}^*$, etc.):

$$\langle E_i^* \rangle P(E_i^*)=4\frac{E_i^*}{\langle E_i^* \rangle}\exp\left[-2\frac{E_i^*}{\langle E_i^* \rangle}\right], \quad i=C^*,P^*,T^* . \tag{1}$$

Here, $\langle E_i^* \rangle$ is the average value of E_i^*. This means, the distribution of the total internal energy of the created clusters in any one of the systems C^*, P^*, and T^* can be determined, provided that the corresponding average value is known. This is in good agreement with the observed[8] properties of the "total transverse energy $E_\perp$" (the sum of $\epsilon_j \sin\theta_j$ where ϵ_j is the energy, and θ_j the scattering angle of the jth observed particle) in the central rapidity region. In fact, it has been shown (see footnote 20 of the first paper in Ref. 4) that

$$\langle E_\perp \rangle P(E_\perp)=4\frac{E_\perp}{\langle E_\perp \rangle}\exp\left[-2\frac{E_\perp}{\langle E_\perp \rangle}\right] . \tag{2}$$

While Eq. (2) is evidently a strong experimental support for assumption (i), the validity of this formula in such a large pseudorapidity range indicates that the carriers of $E_\perp$, namely, the created clusters, are more or less equally distributed in a rapidity range of comparable size—in accordance with assumption (ii).

In order to compare this model with experiments in which charged hadrons are observed, we adopt the usual picture for hadronic clusters[6] as a working ansatz.

The clusters formed in the systems C^*, P^*, and T^* are charge-neutral hadronic objects (color singlets) of approximately the same size. They decay isotropically (with respect to their own rest frame) into a small group of hadrons (e.g., $\pi^+\pi^-\pi^0$, $p\bar{p}$, etc.).

It is well known that the formation and decay of such clusters[6] are consistent with the experimental findings[9] concerning short-range rapidity correlations and local charge compensation. Note that this ansatz also implies that the number of clusters N_i and the number of charged hadrons n_i produced by the system i $(i=C^*,P^*,T^*)$ are proportional to the materialization energy E_i^* of the system. That is,

$$\frac{E^*}{\langle E_i^* \rangle}=\frac{N_i}{\langle N_i \rangle}=\frac{n_i}{\langle n_i \rangle} , \tag{3}$$

where $\langle N_i \rangle$ and $\langle n_i \rangle$ are the average values of N_i and n_i, respectively.

From Eqs. (1) and (3) we obtain

$$\langle n_i\rangle P(n_i)=4\frac{n_i}{\langle n_i\rangle}\exp\left[-2\frac{n_i}{\langle n_i\rangle}\right], \quad i=C^*,P^*,T^* , \tag{4}$$

where $P(n_i)$ is the probability that the system i produces n_i charged particles. It means, in particular, that in the central rapidity region, in which the products of the C^* system dominate, the multiplicity distribution should have the form given by Eq. (4). It also tells us that, in order to obtain the multiplicity distribution in the entire kinematical range we have to take the contributions of C^*, P^*, and T^* into account. (See the first part of Appendix B.) This offers a simple explanation[4] for the experimental observation[5] that KNO scaling is approximately valid in a given central rapidity region, but violated in the entire rapidity space.

III. MULTIPLICITY DISTRIBUTIONS IN DIFFERENT RAPIDITY INTERVALS

We now calculate the multiplicity distributions—including the higher moments—in different rapidity intervals and compare them with the existing data.[1]

Let us first consider the contributions from the C^* system which gives the dominating contribution, especially in the central rapidity region. The isotropic decay of cluster mentioned in the working ansatz implies that the probability density to observe, at a given rapidity y, a hadron produced by the cluster j (we denote the location of the jth cluster in rapidity space by Y_j) is[6,10]

$$\rho(y,Y_j)=\frac{1}{2\cosh^2(y-Y_j)} . \tag{5}$$

Hence, the probability q_{CW} for a hadron produced by one of the N_c clusters of the system C^* to be in the rapidity interval ("rapidity window") W, $y_l\le y\le y_h$, is

$$q_{CW}=\int_{y_l}^{y_h}dy\frac{1}{Y_{C\max}-Y_{C\min}}\int_{Y_{C\min}}^{Y_{C\max}}dY\frac{1}{2\cosh^2(y-Y)} . \tag{6}$$

Here, $Y_{C\min}$ and $Y_{C\max}$ are the kinematical limits for the rapidity of the clusters in system C^*. They can be determined by a simple method given in Appendix B. Expressions similar to that in Eq. (6) can also be obtained for the probability q_{PW} (q_{TW}) for observing a hadron produced by one of the clusters in the system P^* (T^*) in a given rapidity interval. Note that the contributions from P^* and T^* are relatively unimportant unless we consider rapidity intervals far away from the central region. We therefore neglect these contributions in calculating the multiplicity distributions.

Hence, in the approximation in which every cluster is assumed to contain one positively and one negatively charged hadrons, the probability of observing n_W (either positively or negatively) charged hadrons in the rapidity window W is

$$P_W(n_W)=\sum_{N_C}P(N_C)\frac{N_C!}{(n_W/2)!(N_C-n_W/2)!}\times q_{CW}{}^{n_W/2}(1-q_{CW})^{N_C-n_W/2} . \tag{7}$$

Here, $P(N_C)$ is the probability for the system C^* to have N_C clusters. Because of the simple relationship shown in Eq. (3) ($N_C=n_C/2$ in this special case), $P(N_C)$ has the same form as that given in Eq. (4). We recall that the binomial distribution as used in Eq. (7) is the simplest nontrivial discrete distribution for two possible outcomes. Whether the simplest possibility is indeed realized in nature has, however, to be checked experimentally.

First, we see that Eq. (7) implies

$$P_W(n_W)\to P(N_C) \quad \text{for } q_{CW}\to 1 . \tag{8}$$

That is, if the rapidity window W in the central rapidity region is, on the one hand, large enough to include all the hadrons produced by the system C^* but, on the other hand, not too large so that the contributions from the P^* and T^* systems are negligible, the multiplicity distribution $P_W(n_W)$ is expected to satisfy

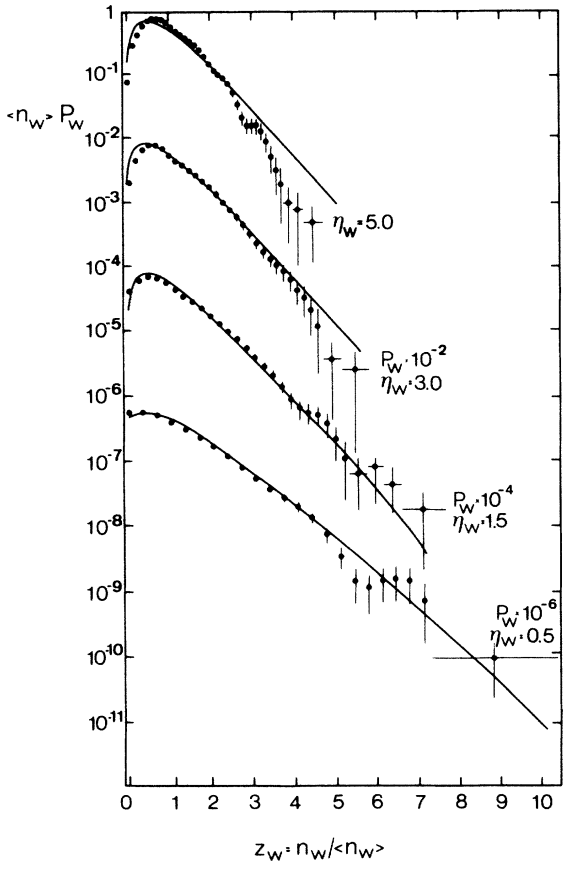

FIG. 2. Charged multiplicity (n_W) distributions in the pseudorapidity intervals ("windows") $|\eta|<\eta_W=5.0$, 3.0, 1.5, and 0.5, plotted in the variables $\langle n_W\rangle P_W(n_W)$ vs $Z_W=n_W/\langle n_W\rangle$. Here $\langle n_W\rangle$ is the average value of n_W, and $P_W(n_W)$ is the probability of observing n_W charged hadrons inside the window $W=2\eta_W$. The data ($\sqrt{s}=540$ GeV) are taken from Ref. 1. The curves are calculated from Eq. (7). Note that in this equation only contributions from the C^* system have been included. Here, as well as in the following figures, rapidities are approximated by pseudorapidity in order to compare with the existing data.

$$\langle n_W \rangle P_W(n_W) = 4 \frac{n_W}{\langle n_W \rangle} \exp\left[-2 \frac{n_W}{\langle n_W \rangle} \right], \quad (9)$$

where $\langle n_W \rangle$ is the average value of n_W in the rapidity window W. It means, in particular, that for every given (total c.m.s.) energy $\sqrt{s}$ (sufficiently high so that the overlapping regions of C^* with P^* and T^* systems in rapidity space are relatively small) there is a rapidity interval W in which the probability $P_W(n_W)$ to find n_W charged hadrons in the interval W satisfies Eq. (9). The size of this particular rapidity interval at a given energy can be estimated by the method given in Appendix B. It is approximately $|y| \leq 1.5$ for $\sqrt{s} = 63$ GeV, $|y| \leq 3$ for $\sqrt{s} = 540$ GeV.

In Fig. 2 we show the result calculated from Eq. (7) for $\sqrt{s} = 540$ GeV and the following rapidity intervals: $|y| < y_W = 5$, 3, 1.5, and 0.5. The results are given in terms of the scaled variables $n_W/\langle n_W \rangle$, where $\langle n_W \rangle$ is the average value of n_W in the interval W. The data points are those published by the UA5 Collaboration[1] for the pseudorapidity intervals $|\eta| < \eta_W = 5$, 3, 1.5, and 0.5. The comparison shows that the measured distribution $\langle n_W \rangle P(n_W)$ has indeed the form given by Eq. (9) provided that the rapidity interval in which the measurement is made is not too far away from $y_W \approx \eta_W = 3$. It also shows that Eq. (7) gives a good description of the data for $\eta_W \leq 3$. The discrepancy at $\eta_W = 5$ is due to the neglect of the P^* and T^* systems. We note, in particular, the two observed[1] characteristic features of rapidity-interval dependence mentioned in the Introduction of this paper are nicely reproduced by this formula.

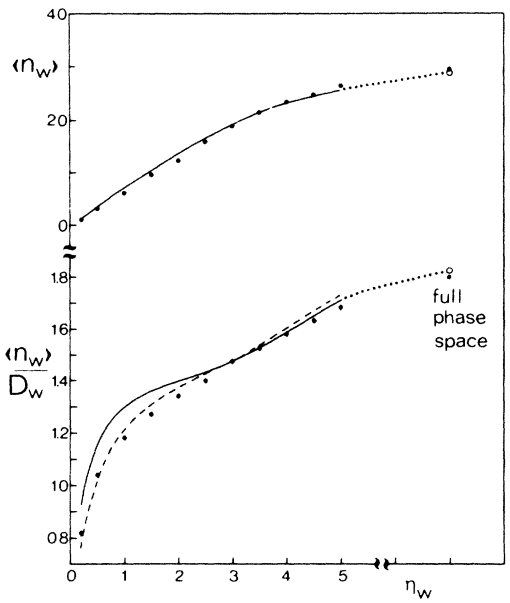

FIG. 3. The average multiplicity $\langle n_W \rangle$ of charged hadrons in a given pseudorapidity window $|\eta| < \eta_W$, and the ratio $\langle n_W \rangle / D_W$ where $D_W = \langle (n_W - \langle n_W \rangle)^2 \rangle^{1/2}$, as functions of η_W. The data points ($\sqrt{s} = 540$ GeV) are taken from Ref. 1. The curves are the calculated results of this model. (See Appendix C for details.) The dashed curves represent the calculations in which the corresponding multiplicity distributions are normalized up to the last measured points (with the largest multiplicities in the window W), while the solid curves are those in which such normalization effects due to measurements are neglected. Whenever the dashed and the solid curves coincide, only the solid one is drawn. The dotted line is given merely to guide the eye.

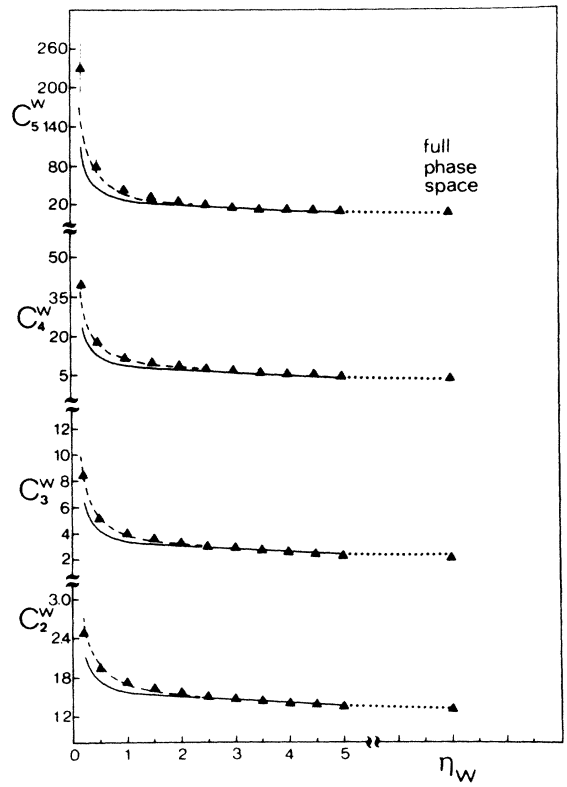

FIG. 4. The moments $C_l^W = \langle n_W{}^l \rangle / \langle n_W \rangle^l$, for $l = 2$, 3, 4, and 5, of the multiplicity distributions of charged hadrons in the rapidity window $|\eta| < \eta_W$, as functions of η_W. The data points ($\sqrt{s} = 540$ GeV) are taken from Ref. 1. The curves are the results of this model. Here the dashed, solid, and the dotted lines have the same meaning as those in Fig. 3.

In Figs. 3 and 4 we compare the calculated average multiplicities, dispersions as well as higher moments in different rapidity intervals with those measured experimentally.[1] The contributions of the P^* and T^* system are taken into account. The details of this calculation is given in Appendix C.

The calculated and the measured moments of the multiplicity distributions in noncentral rapidity intervals are compared in Fig. 5. It should be pointed out that the following experimental fact is one of the characteristic properties of this statistical model. The moments of the multiplicity distributions are approximately independent of the location of the rapidity interval provided that it remains in the central rapidity region.

In Fig. 6 and Table I we show the calculated results for the same set of rapidity windows for different c.m.s. energies. The data are taken from Refs. 11–13. The predictions are based on this model under the same conditions as those mentioned in Ref. 10 (for details see Appendix B): (a) The average multiplicities of the P^* (and the T^*)

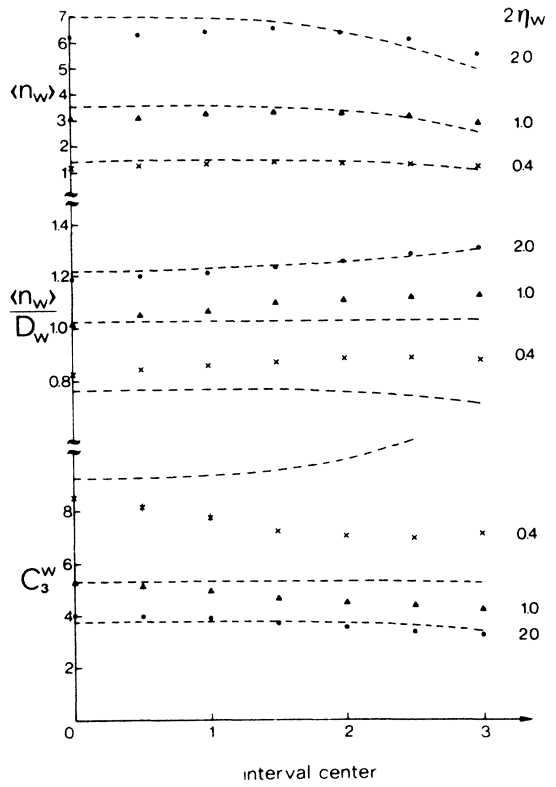

FIG. 5. The average multiplicity $\langle n_W \rangle$, the ratio $\langle n_W \rangle / D_W$, and the third moment C_3^W in the pseudorapidity windows of size $2\eta_W = 0.4$, 1.0, and 2.0 in noncentral intervals, as functions of the interval center. The data points ($\sqrt{s} = 540$ GeV) are taken from Ref. 1. The dashed curves are the calculated results, normalized in the same manner as in Fig. 3.

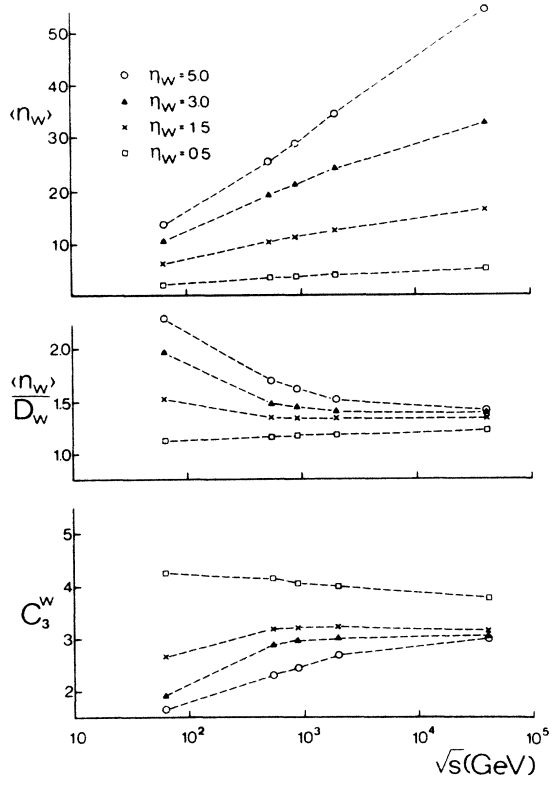

FIG. 6. The calculated results of $\langle n_W \rangle$, $\langle n_W \rangle / D_W$, and C_3^W for four different pseudorapidity windows: $|\eta| < \eta_W = 0.5$, 1.5, 3.0, and 5.0, as functions of the total c.m.s. energy $\sqrt{s}$. The normalization effect due to measurements mentioned in Fig. 3 is not taken into account. The broken lines are drawn to guide the eye.

TABLE I. Energy dependence of the normalized charged-multiplicity moments, which are defined as follows: $\gamma_2^W = \langle (n_W - \langle n_W \rangle)^2 \rangle / \langle n_W \rangle^2$, $\gamma_3^W = \langle (n_W - \langle n_W \rangle)^3 \rangle / \langle n_W \rangle^3$, $\gamma_4^W = \langle (n_W - \langle n_W \rangle)^4 \rangle / \langle n_W \rangle^4 - 3(\gamma_2^W)^2$. The experimental data are taken from Refs. 11–13.

$\sqrt{s}$ (GeV)		γ_2^W	γ_3^W	γ_4^W
53	Model	0.38	0.28	0.34
	Expt. (Ref. 11)	0.45 ±0.01	0.37 ±0.02	0.37 ±0.06
63	Model	0.41	0.31	0.45
	Expt. (Ref. 11)	0.46 ±0.01	0.28 ±0.02	0.29 ±0.05
540	Model	0.54	0.57	0.89
	Expt. (Ref. 12)	0.52 ±0.01	0.53 ±0.05	0.80 ±0.18
	Expt. (Ref. 13)	0.441±0.017	0.308±0.021	0.216±0.050
900	Model	0.55	0.57	0.90
2000	Model	0.55	0.57	0.90
40000	Model	0.55	0.57	0.90

systems, which turned out to be the same at $\sqrt{s}=63$ and 540 GeV, remain the same also at higher energies. (b) The empirical formula for the averaged multiplicity of charged hadrons $n_{\rm ch}=a+b\ln s+c(\ln s)^2$ with a,b,c given by the UA5 Collaboration[1] is valid also at high energies.

Rapidity distributions at different energies have already been calculated in the framework of this model.[14,15] In particular, a flat rapidity distribution for the produced particles has been used in Ref. 15. Discussions on this and other related topics will therefore not be repeated here.

IV. LONG-RANGE CORRELATIONS

We now consider the long-range correlation between the forward and backward multiplicities, n_F and n_B, of charged hadrons measured in the following rapidity intervals ($-b\le y\le -a$; $a\le y\le b$) where a and b are positive real constants. Experimentally, there exist data at $\sqrt{s}=540$ GeV (Ref. 2) and at all five standard CERN ISR energies[3] for $(a,b)=(0,4)$, $(0,1)$, $(1,4)$, ... Hereafter we shall denote rapidity regions $-b\le y\le -a$ and $a\le y\le b$ by B and F, respectively, denote the rest of the kinematically allowed rapidity region by R, and denote the number of charged hadrons in R by n_R. That is, the total number of prongs in a collision event is $n=n_B+n_F+n_R$.

According to the discussions which led us to Eq. (6), the probabilities q_{CB}, q_{CF}, and q_{CR} for a charged hadron produced by C^* to be in B, F, and R can be written as follows:

$$q_{CB}=\int_{-b}^{-a}dy\frac{1}{Y_{C\max}-Y_{C\min}}\int_{Y_{C\min}}^{Y_{C\max}}dY\frac{1}{2\cosh^2(y-Y)}\ , \tag{10a}$$

$$q_{CF}=\int_{a}^{b}dy\frac{1}{Y_{C\max}-Y_{C\min}}\int_{Y_{C\min}}^{Y_{C\max}}dY\frac{1}{2\cosh^2(y-Y)}\ , \tag{10b}$$

$$q_{CR}=1-q_{CB}-q_{CF}\ . \tag{10c}$$

Here $Y_{C\min}$, and $Y_{C\max}$ have the same meaning as those in Eq. (6). It is clear that also in Eqs. (10a)–(10c) only contributions from C^* have been taken into account. Those from P^* and T^* can be included in a straightforward manner. But it is expected that they will not have much influence on the final result, except when the total

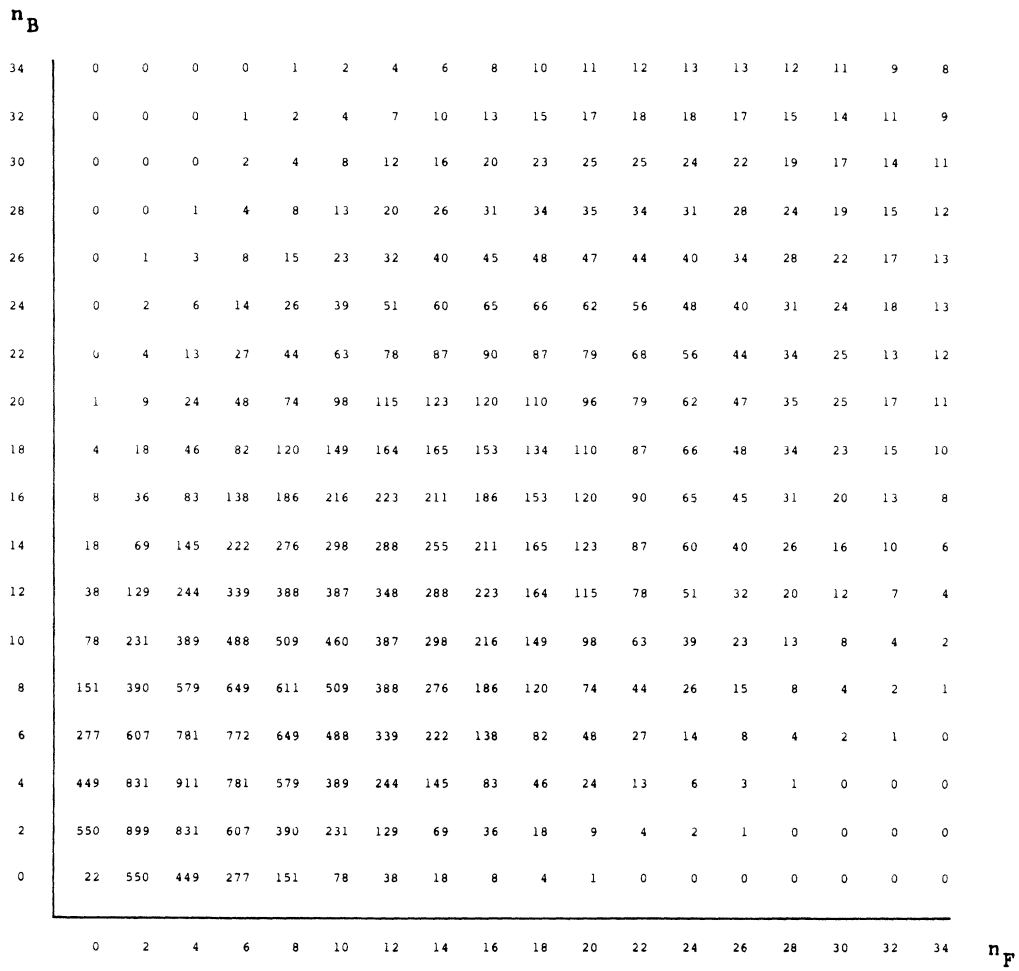

FIG. 7. The calculated scatter plot of multiplicities n_B and n_F for the pseudorapidity intervals B ($-4<\eta<0$) and F ($0<\eta<4$). The plot is normalized in an arbitary scale. Comparison with the corresponding data in Ref. 2 shows that it has indeed the same structure.

c.m.s. energy of the system is so low that the central system C^* loses its dominating role (see Appendix B) or when the (pseudo)rapidity gap between the F and the B regions is very large (≥ 6, for example).

Since there are three possible outcomes (with probabilities q_{CB}, q_{CF}, and q_{CR}) for every (positively or negatively) charged hadron in any (high-energy nondiffractive hadron-hadron collision) event, the random variable is a three-dimensional vector $(n_B/2, n_F/2, n_R/2)$, but the range of values is restricted to a two-dimensional, e.g., (n_B, n_F), space because of $n_B+n_F+n_R=n_C$, where $n_C/2$ is the number of positively (or negatively) charged hadrons produced by the central system C^*. [Recall that in the approximation in which each cluster is assumed to contain one positively and one negatively charged hadron, $n_C/2=N_C$ is the number of clusters in the system C^*. From Eqs. (3) and (4) we know that the cluster distribution $P(N_C)$ should have the same form as that given in Eq. (4).] The distribution $Q(n_B,n_F)$ in the two-dimensional (n_B,n_F) space is assumed to be a trinomial:

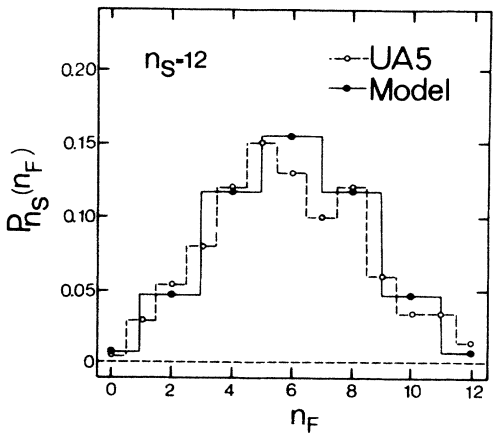

FIG. 8. Comparison between experiment and theory for the n_F distribution for a given value of n_s. Data are those given in Ref. 2. Black dots and the solid line are the results of our calculation.

$$Q(n_B,n_F)=\sum_{N_C\geq(n_F+n_B)/2} P(N_C)\frac{N_C!}{(n_B/2)!(n_F/2)![N_C-(n_B+n_F)/2]!}q_{CB}^{n_B/2}\,q_{CF}^{n_F/2}\,q_{CR}^{[N_C-(n_B+n_F)/2]} \tag{11}$$

which, as we know, is the simplest nontrivial discrete distribution for the three possible outcomes.

In order to see whether nature *indeed* chose the simplest possibility, we first calculate this joint distribution $Q(n_B,n_F)$. This is because, if the model is correct, $Q(n_B,n_F)$ should be nothing else but the scatter plot in which $n_B/2$ and $n_F/2$ are the positively (or negatively) charged hadrons observed in the corresponding B and the F regions in rapidity space, respectively. To compare with the published data[2] for the (n_B,n_F) plot, the calculated $Q(n_B,n_F)$ is shown in Fig. 7. In Fig. 8 we compare the measured n_F distribution for $n_B+n_F=12$ in the rapidity interval $(a,b)=(0,4)$, with the corresponding result obtained from Eq. (11). Furthermore, the average value of n_B for a given n_F can be readily obtained from

$$\langle n_B(n_F)\rangle=\frac{\sum_{n_B=0,2,\ldots} n_B Q(n_B,n_F)}{\sum_{n_B=0,2,\ldots} Q(n_B,n_F)} \tag{12}$$

and Eq. (11). The comparison with the data at $\sqrt{s}=540$ and 63 GeV for different rapidity intervals is shown in Figs. 9–11. In particular, as we can see from Fig. 11, for a given energy the strength of long-range correlations becomes weaker and weaker when the separation between the two rapidity windows increases. This kind of

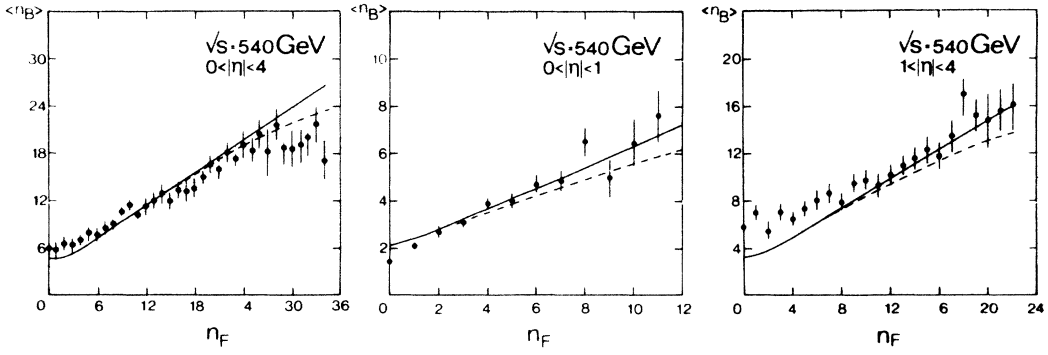

FIG. 9. The dependence of $\langle n_B(n_F)\rangle$, the average value of n_B as a function of n_F are shown in three different pseudorapidity intervals at total c.m.s. energy $\sqrt{s}=540$. Data are taken from Ref. 2. Dashed lines are again those in which the normalization effect due to measurements are taken into account (cf. Fig. 3).

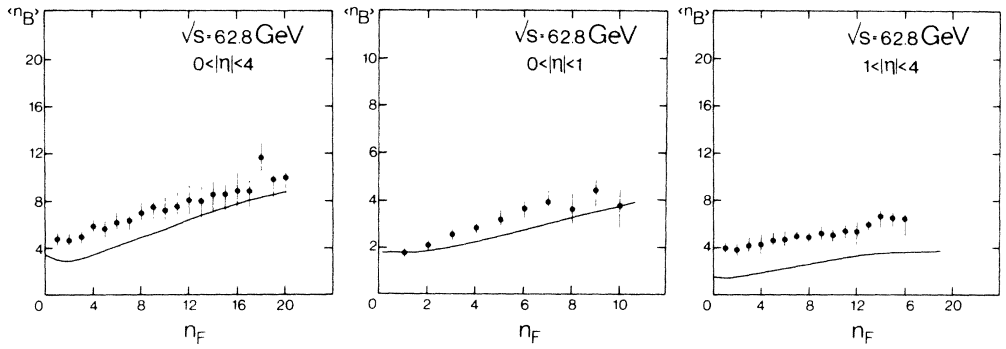

FIG. 10. $\langle n_B(n_F)\rangle$ as a function of n_F in different pseudorapidity intervals at the highest CERN ISR energy ($\sqrt{s}=63$ GeV). Data are taken from Ref. 3. The discrepancy in absolute values (but not in the slope) for the interval $1<|\eta|<4$ is expected. It is due to the fact that at such low energies the contributions from the P^* and T^* systems become significant in these pseudorapidity regions.

behavior is expected and has been discussed in Ref. 4.

Last but not least, we show (in Appendix D) that simple relations exist between the following measurable quantities: the sum of the charged multiplicities in the F and the B region $n_s=n_F+n_B$, the dispersion $d_s^2(n_F)$ of the distribution describing the probability of finding events with n_F charged hadrons in the F region for fixed n_s, and/or the average value of $\langle Z^2\rangle_s$ for fixed n_s where $Z=n_F-n_B$. They are

$$d_s^2(n_F)=n_s/2\ , \tag{13}$$

$$\langle Z^2\rangle_s=2n_s\ . \tag{14}$$

As we can see from the proof given in Appendix D, the validity of Eqs. (13) and (14) is *independent of the size of the B and the F regions* and it is also *independent of whether or not there is a gap between these two regions,* provided that the dominating contributions in these two regions remain to be those of the system C^*. Experimental data[2] of the UA5 Collaboration for various sizes of B and F region seems to indicate that it is indeed the case. This is shown in Fig. 12.

The following should be pointed out in connection with Eqs. (11)—(14).

(a) Predictions for higher energies can be made under the same conditions as those mentioned in Sec. III. They are shown in Figs. 13 and 14.

(b) In the special case $(a,b)=(0,y_{\max})$, where $y_{\max}$ is the kinematical limit of the rapidity space at the given total c.m.s. energy $\sqrt{s}$, that is, when the F and B regions are identical with the entire kinematically allowed for-

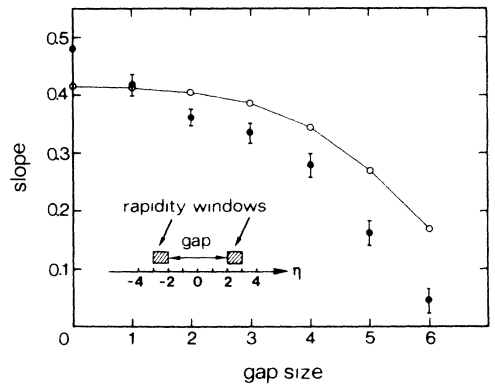

FIG. 11. The dependence of the slope of the linear fit for $\langle n_B(n_F)\rangle$ as a function of n_F on the size of the rapidity gap. The values obtained from the data are taken from Carlson's talk in Ref. 2. They are shown as ● in the figure. The corresponding theoretical values are shown as ○. Note that, since the $\langle n_B\rangle$ vs n_F curves in our model are not necessarily straight lines, the slope is obtained by a straight-line approximation of the curve.

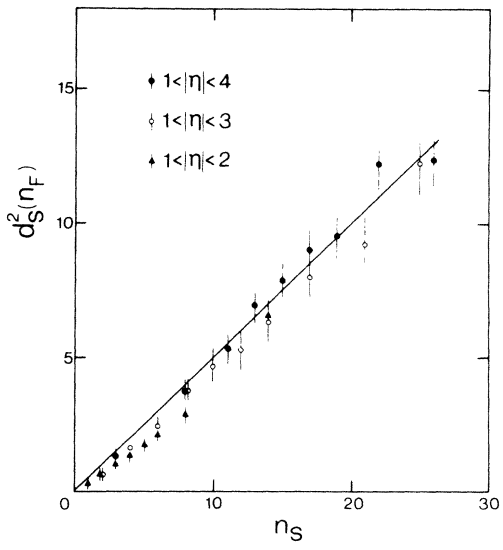

FIG. 12. The dispersion d_s squared as a function of n_s for three different forward-backward regions each with a gap $(-1<\eta<1)$ between them. The size of the regions are given in the figure. The curve is obtained from Eq. (13).

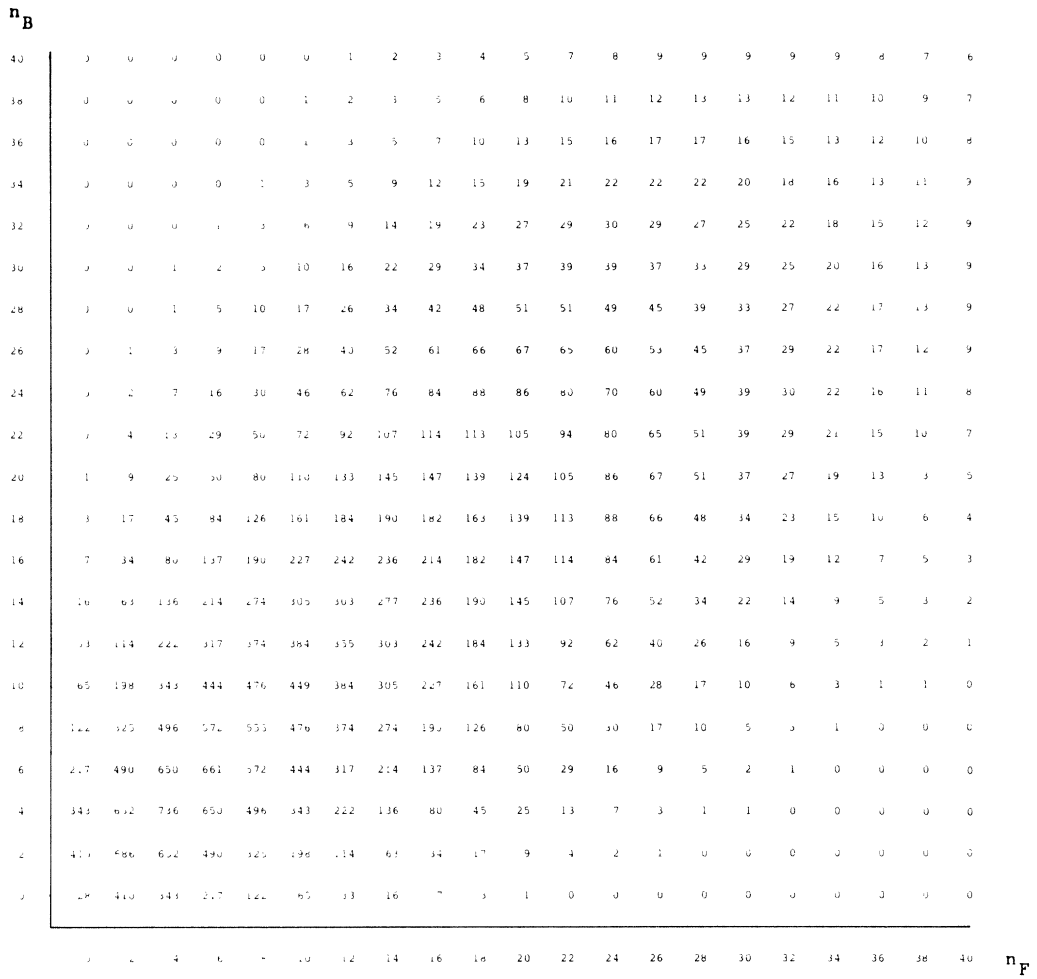

FIG. 13. Our prediction for the n_B vs n_F scatter plot at c.m.s. energy $\sqrt{s}=900$ GeV. Here, the B and F regions are also taken to be $(-4<\eta<0)$ and $(0<\eta<4)$, respectively. The normalization is made in an arbitrary scale.

ward and backward hemisphere, respectively, $Q(n_B,n_F)$ reduces to a binomial distribution. Binomial distributions as well as cluster formation[6] have been discussed by the UA5 Collaboration[2,5] and by Chou and Yang.[16] In this special case the difference between their results and ours is only that the n_s distribution in our model is given by the expression in Eq. (4).

(c) The simple relationship between $\langle Z^2\rangle_s$ and n_s given in Eq. (14) was first obtained by Chou and Yang[16] by analyzing the UA5 data.[2] They also pointed out the significance and the physical meaning of the factor 2 in that formula. In our model, local charge neutrality is guaranteed by the usual[6] assumption that the clusters are charge neutral objects. Furthermore, Eq. (14) is a direct consequence of Eq. (11). As shown in Appendix D, the simple relationship is true also in cases where there is a large rapidity gap between the B and the F regions.

(d) We expect to see that long-range correlations in pion- and kaon-nucleon reactions at comparable energies will be the *same* as those discussed here. This is because, in our model, the projectile-target asymmetry (viewed from the total c.m.s. frame) only effects the leading particles but not the systems C^*, P^*, and T^*.

V. CONCLUDING REMARKS

A number of theoretical models[17] have been proposed to understand the multiplicity distributions measured[5] at $\sqrt{s}=540$ GeV. Some of the calculated results are rather similar although the underlying physical pictures are very much different from one another. The new UA5 multiplicity measurements[1] in different rapidity intervals as well as such experimental data at higher energies are expected to be able to differentiate between the competing models.[17,4] It is with this hope that we made the present

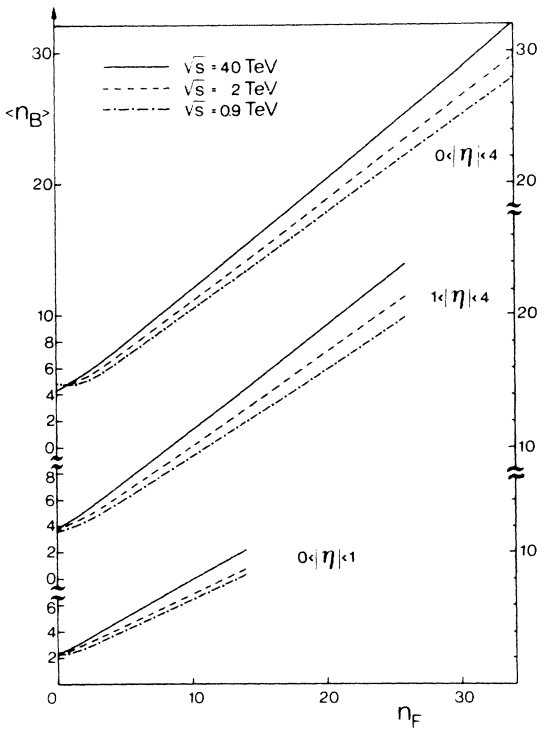

FIG. 14. Our predictions for the dependence of $\langle n_B(n_F)\rangle$ as functions of n_F for three different pseudorapidity regions at c.m.s. energies $\sqrt{s}=900$ GeV, 2 and 40 TeV.

attempt and calculated in terms of our model the multiplicity distributions and long-range correlations for various rapidity intervals at $\sqrt{s}=540$ GeV as well as those at higher energies.

ACKNOWLEDGMENTS

The authors wish to thank their colleagues in Beijing, Berlin, Jinan, and Wuhan, especially Liu Lian-sou who took part in the initial stage of this work during his visit in Berlin, for many helpful discussions. They are grateful to G. Ekspong for calling to their attention the important role of cluster distribution in such processes, and to T. T. Wu for his critical remarks concerning the nonquantum aspects of this model. This work was supported in part by Deutsche Forschungsgemeinschaft and Max-Planck Gesellschaft.

APPENDIX A

We consider any one of the three systems i ($i=C^*,P^*,T^*$). Let us denote, for the sake of simplicity, the materialization energy E_i^* of this system by E, the two energy-momentum sources of this system by 1 and 2. Let $f_1(E_1)$ be the probability for the system i to obtain an amount E_1 from source 1, and $f_2(E_2)$ that for the system i to obtain E_2 from source 2. Then, since the two sources 1 and 2 are independent from each other, the probability $f(E_1,E_2)$ for i to obtain E_1 from source 1 and E_2 from source 2 is simply the product $f_1(E_1)f_2(E_2)$. Now, if this probability $f(E_1,E_2)$ depends only on E, the sum of E_1 and E_2, but independent of E_1 or E_2 [assumption (i)], we have

$$\frac{d}{dE_1}[f_1(E_1)f_2(E-E_1)]=0\ . \tag{A1}$$

Hence

$$\frac{d}{dE_1}[\ln f_1(E_1)]-\frac{d}{d(E-E_1)}[\ln f_2(E-E_1)]=0\ , \tag{A2}$$

which gives

$$f_1(E_1)=A_1\exp(-BE_1)\ , \tag{A3}$$

$$f_2(E_2)=A_2\exp(-BE_2)\ , \tag{A4}$$

where A_1, A_2, and B are positive real numbers. (We recall that f_1 and f_2 are probabilities.) Therefore, the probability for the system i to be in the state characterized by the total materialization energy E is

$$\begin{aligned}P(E)&=\int dE_1dE_2\delta(E-E_1-E_2)f_1(E_1)f_2(E_2)\\&=\int_0^E dE_1A_1A_2\exp(-BE)\\&=A_1A_2E\exp(-BE)\ .\end{aligned} \tag{A5}$$

Taken together with the normalization condition

$$\int P(E)dE=1\ , \tag{A6}$$

and the definition for the average value of E,

$$\int EP(E)dE=\langle E\rangle\ , \tag{A7}$$

we obtain

$$P(E)=4\frac{E}{\langle E\rangle^2}\exp\left[-2\frac{E}{\langle E\rangle}\right] \tag{A8}$$

which is Eq. (1) in the text.

APPENDIX B

According to our model[4] the multiplicity distribution for charged hadrons observed in the entire kinematically allowed rapidity region in nondiffractive processes is (the approximation that each cluster is assumed to contain one positively and one negatively charged hadron will also be used in this appendix as well as in Appendix C)

$$P(n_{\rm ND})=\int 2\delta(n_C+n_P+n_T-n_{\rm ND})\prod_{i=C^*,P^*,T^*}P(n_i)dn_i\ , \tag{B1}$$

where the subscript ND in $n_{\rm ND}$ stands for nondiffractive and the average values of n_i, $\langle n_i\rangle$ ($i=C^*,P^*,T^*$) in $P(n_i)$ are given by

$$\langle n_C\rangle=\alpha\langle n_{\rm ND}\rangle,\ \ \langle n_P\rangle=\langle n_T\rangle=\frac{1-\alpha}{2}\langle n_{\rm ND}\rangle\ ; \tag{B2}$$

α is an energy-dependent parameter. In fact, it is found[10,14] that α increases monotonically with increasing energy. Its values is between 0.15 and 0.5 for $14<\sqrt{s}<63$ GeV, and becomes 0.75 for $\sqrt{s}=540$ GeV.

Comparisons between experiments[5] and theory are shown in Refs. 10 and 11. The following observations have been made in this connection.

(1) The scaling behavior of $\langle n_{\rm ND}\rangle P_{\rm ND}(n_{\rm ND})$ with respect to $n_{\rm ND}/\langle n_{\rm ND}\rangle$ observed experimentally in the energy range $14<\sqrt{s}<63$ GeV is due to the fact that this expression is insensitive to the variation of α for $0.15<\alpha<0.5$.

(2) By using the values $\alpha=0.5$ for $\sqrt{s}=63$ GeV, $\alpha=0.75$ for $\sqrt{s}=540$ GeV and experimental values for $\langle n_{\rm ND}\rangle$, the product $(1-\alpha)\langle n_{\rm ND}\rangle$ calculated at these two energies turns out to be the same (≈ 7). That is, the average multiplicity of the P^* and that of the T^* system are the same for $\sqrt{s}=63$ and 540 GeV. This result is also in agreement with the hypothesis of limiting fragmentation.

(3) Based on the observation mentioned in (2) we assume

$$[1-\alpha(s)]\langle n_{\rm ND}\rangle = 7 \quad \text{for all } \sqrt{s} > 63 \text{ GeV} . \tag{B3}$$

This can be used to determine the s dependence of α if that of $\langle n_{\rm ND}\rangle$ is known. Hence, by extrapolating the empirical formula [e.g., $\langle n_{\rm ND}\rangle = a + b\ln s + c(\ln s)^2$ where a, b, and c are constant[1,5]] we are able to calculate, in particular, $\langle n_C\rangle$ as a function of the total c.m.s. energy $\sqrt{s}$.

On the other hand, it is clear that $\langle n_C\rangle$ is closely related to the average multiplicity density in the central rapidity region. In fact, from assumption (ii) which states that the clusters in system C^* are uniformly distributed in the rapidity region $Y_{C\min}\le Y\le Y_{C\max}$, we see that average width of this distribution $Y_{C\max}-Y_{C\min}(=2Y_{C\max}$ in the c.m. system) can be obtained from

$$2Y_{C\max}\left[\frac{dn}{dy}\right]_{y=0} = \langle n_C\rangle , \tag{B4}$$

where $(dn/dy)_{y=0}$ is the average multiplicity density near $y=0$ in the c.m. system.

Hence, from Eqs. (B3) and (B4), we can calculate $Y_{C\max}$ for all c.m.s. energies, provided that $\langle n_{\rm ND}\rangle$ and $(dn/dy)_{y=0}$ at these energies are known. By using the measured $(dn/dy)_{y=0}$ values[5] and the known values for $\langle n_{\rm ND}\rangle$ (Refs. 1 and 5) at $\sqrt{s}=63$ and 540 GeV, we have $Y_{C\max}\approx 1.5$ for $\sqrt{s}=63$ GeV and $Y_{C\max}\approx 3$ for $\sqrt{s}=540$ GeV.

Furthermore, the average width of the cluster distribution in the C^* system obtained by the above-mentioned method can also be used to determine the corresponding rapidity window $y_W=Y_{C\max}$ in which the multiplicity distribution obeys Eq. (9). The reason is obvious. Using the two values of $Y_{C\max}$ at $\sqrt{s}=540$ and 63 GeV as input, a two-parameter fit for $Y_{C\max}$ as a function of c.m.s energy $\sqrt{s}$ can be obtained:

$$Y_{C\max} = c + d\ln s , \tag{B5}$$

where $c=-1.37$ and $d=0.347$. From Eq. (B5) we can then predict the size of rapidity window at any given c.m.s. energy $\sqrt{s}$, inside which the multiplicity distribution has the simple form given by Eq. (9).

APPENDIX C

When the rapidity windows are large ($|y| \gg Y_{C\max}$, for example) it is not sufficient to consider only the contributions of the C^* system especially in calculating the higher moments. The contributions of the P^* and the T^* system can, in general, be included in the following way.

From Appendix B we know the following. First, at a given c.m.s. energy $\sqrt{s}$ the average multiplicity of the clusters in the systems C^*, P^*, and T^* are $\langle n_C\rangle/2$, $\langle n_P\rangle/2$, and $\langle n_T\rangle/2$, respectively. They are related to the measured multiplicity of the charged hadrons in nondiffractive hadron-hadron processes $\langle n_{\rm ND}\rangle$ through Eq. (B2). Second, for the system C^*, the average width of the cluster distribution in rapidity space can be estimated. It is given by Eq. (B5). Let us now denote the average width of the P^* and the T^* system by $\Delta_P=\Delta_T=\Delta$ (the average values are equal because of the symmetry). Since the clusters in each of the three systems are distributed with equal probability in its own rapidity region, and the leading particles, on the average, take away half of the total c.m.s. energy while the rest is distributed in the three excited systems C^*, P^*, and T^*, energy conservation requires

$$\begin{aligned}\sqrt{s} = {} & \frac{\langle n_T\rangle}{\Delta}\int_{Y_{T\min}}^{Y_{T\max}} m^*\cosh y\, dy \\ & + \frac{\langle n_C\rangle}{Y_{C\max}-Y_{C\min}}\int_{Y_{C\min}}^{Y_{C\max}} m^*\cosh y\, dy \\ & + \frac{\langle n_P\rangle}{\Delta}\int_{Y_{P\min}}^{Y_{P\max}} m^*\cosh y\, dy .\end{aligned} \tag{C1}$$

Here

$$\begin{aligned} & Y_{T\max}=Y_{C\min},\quad Y_{T\min}=Y_{C\min}-\Delta , \\ & Y_{P\max}=Y_{C\max}+\Delta,\quad Y_{P\min}=Y_{C\max} ,\end{aligned} \tag{C2}$$

and m^* is the average internal energy of a cluster. [We used the approximation

$$m^* = 3(m_\pi{}^2+\tfrac{3}{2}\bar{p}_\perp{}^2)^{1/2} ,$$

where $\bar{p}_\perp$ is the average transverse momentum of the observed hadron in our calculation.] The average width Δ can be obtained by solving Eq. (C1).

The probability q_{iW} for hadron produced by one of the N_i clusters in the system i ($i=C^*$, P^*, or T^*) to be in a certain rapidity interval W ($y_l\le y\le y_h$) is

$$q_{iW} = \int_{y_l}^{y_h} dy \frac{1}{Y_{i\max}-Y_{i\min}}\int_{Y_{i\min}}^{Y_{i\max}} dY \frac{1}{2\cosh^2(y-Y)} . \tag{C3}$$

Hence the probability to have n_W hadrons in this rapidity interval can be expressed as

$$F(n_W)=\sum_{N_C,N_P,N_T} P(N_C)P(N_P)P(N_T) \sum_{\substack{n_{CW},n_{PW},n_{TW} \\ (n_{CW}+n_{PW}+n_{TW}=n_W)}} B_C(N_C,n_{CW})B_P(N_P,n_{PW})B_T(N_T,n_{TW}) , \tag{C4}$$

where $P(N_i)$ is the distribution of the cluster number in the system i, and

$$B_i(N_i,w_{iW})=\begin{bmatrix} N_i \\ n_{iW}/2 \end{bmatrix} q_{iW}^{n_{iW}/2}(1-q_{iW})^{N_i-n_{iW}/2} \tag{C5}$$

is the distribution of cluster number $n_{iW}/2$ inside the rapidity interval W for the system i with total number of clusters N_i.

The lth moment of n_W can be obtained from $F(n_W)$ in Eq. (C4):

$$C_l^W=\langle n_W{}^l\rangle/\langle n_W\rangle^l . \tag{C6}$$

Note that the moments for $P(N_i)$ and B_i can be given analytically. In fact, C_l^W can be expressed in terms of the moments of $P(N_i)$ and B_{iW} through a straightforward calculation.

APPENDIX D

We consider $Q(n_B,n_F)$ as given in Eq. (11) as a function of $n_s=n_B+n_F$ and n_F. Under this variable transformation, Eq. (11) can be rewritten as

$$Q(n_s-n_F,n_F)=\sum_{N_C\geq n_s/2} P(N_C)\frac{Nc!}{(n_s-n_F)/2!(n_F/2)!(N_C-n_s/2)!} q_{CB}^{(n_s-n_F)/2} q_{CF}^{n_F/2} q_{CR}^{(N_C-n_s/2)} . \tag{D1}$$

The quantity $d_s{}^2(n_F)$ is by definition

$$d_s{}^2(n_F)=\frac{A_2}{A_0}-\left[\frac{A_1}{A_0}\right]^2 , \tag{D2}$$

where

$$A_0=\sum_{n_F=0,2,\ldots} Q(n_s-n_F,n_F) ,$$

$$A_1=\sum_{n_F=0,2,\ldots} n_F Q(n_s-n_F,n_F) ,$$

$$A_2=\sum_{n_F=0,2,\ldots} n_F{}^2 Q(n_s-n_F,n_F) ,$$

It can be readily shown that

$$\frac{A_1}{A_0}=n_s\frac{q_{CF}}{q_{CB}+q_{CF}} \tag{D3}$$

and

$$\frac{A_2}{A_0}=2n_s\frac{q_{CF}}{q_{CB}+q_{CF}}+n_s(n_s-2)\left[\frac{q_{CF}}{q_{CB}+q_{CF}}\right]^2 . \tag{D4}$$

Furthermore, although q_{CF} and q_{CB} depend on the size of the B and F regions, as well as on the size of the gap between them, the ratio

$$\frac{q_{CF}}{q_{CB}+q_{CF}}=\frac{1}{2} \tag{D5}$$

remains unchanged, because the two regions B and F are equally large and symmetric with respect to $y=0$. From Eqs. (D2)–(D5) we obtain Eq. (13) in the text.

*On leave from Hua-Zhong Normal University, Wuhan, China.
†On leave from Institute of High-Energy Physics, Academia Sinica, Beijing, China.

[1]UA5 Collaboration, G. J. Alner *et al.*, Phys. Lett. **160B**, 193 (1985).

[2]UA5 Collaboration, K. Alpgard *et al.*, Phys. Lett. **123B**, 361 (1983); J. Gaudaen, in *Multiparticle Dynamics, 1982,* proceedings of the XIII International Symposium, Volendam, The Netherlands, edited by W. Kittel, W. Metzger, and A. Stergiou (World Scientific, Singapore, 1982); K. Böckman, in *Proceedings of the Third International Conference on Physics in Collisions, Como, Italy, 1983,* edited by G. Bellini and A. Bettini (Editions Frontières, Gif-sur-Yvette, 1983); P. Carlson, in *Proceedings of the XIth International Winter Meeting on Fundamental Physics, Toledo, Spain, 1983,* edited by A. Ferrando (Instituto de Estudios Nucleares, Madrid, 1983).

[3]S. Uhlig, I. Derado, R. Meinke, and H. Preisner, Nucl. Phys. **B132**, 15 (1978).

[4]Liu Lian-sou and Meng Ta-chung, Phys. Rev. D **27**, 2640 (1983); Chou Kuang-chao, Liu Lian-sou, and Meng Ta-chung, *ibid.* **28**, 1080 (1983).

[5]See, for example, Ref. 2 and G. Ekspong, in *Mesons, Isobars, Quarks, and Nuclear Excitations,* proceedings of the International School of Subnuclear Physics, Erice, 1983 [Progress in Particle and Nuclear Physics, edited by D. Wilkinson (Pergamon, London, 1984), Vol. II]; D. G. Rushbrooke, in *Proceedings of the DPF Workshop on $\bar{p}p$ Options for the Supercollider, Chicago, 1984,* edited by J. Pilcher and A. R. White (Physics Department, University of Chicago, Chicago, 1984); P. Carlson, in *Proceedings of the 4th Topical Workshop*

on Proton-Antiproton Collider Physics, Berne, 1984, edited by H. Hanni and J. Schacher (Report No. CERN-84-39, 1984), as well as the references given therein.

[6]Production of small clusters in connection with the existence of short-range rapidity correlations in high-energy hadron-hadron collisions has been discussed by many authors many years ago. Details and references can be found in the following review articles as well as the papers cited therein: L. Foa, Phys. Rep. **22**, 1 (1975); A. Bialas, in *Proceedings of the IVth International Symposium on Multiparticle Hadrodynamics, Pavia, 1973,* edited by F. Duimio, A. Giovannini, and S. Ratti (Instituto Nationale di Fisica Nucleare, Rome, 1973), p. 93. The relationship between small cluster production and long-range multiplicity correlation has been discussed by J. Benecke and Y. Kühn [Nucl. Phys. **B140**, 179 (1978)] and K. Alpgard *et al.* (UA5 Collaboration, Ref. 2). These authors use empirical KNO scaling function and/or Poisson distribution for cluster multiplicity and uniform distribution for cluster rapidity. The result of their calculation (based on measured KNO functions or by using Monte Carlo simulation) is in good agreement with the data (Refs. 2 and 3).

[7]S. Pokorski and L. Van Hove, Acta Phys. Pol. **B5**, 229 (1974); P. Carruthers and Ming Duong-Van, Phys. Rev. D **28**, 130 (1983).

[8]UA1 Collaboration, G. Arnison *et al.*, CERN Report CERN-EP/82-122, 1982 (unpublished); Phys. Lett. **123B**, 115 (1983).

[9]See, for example, the following: L. Foa, in Ref. 6; G. Gacomelli, and M. Jacob, Phys. Rep. **55**, 1 (1979), and papers cited therein.

[10]Cai Xu and Liu Lian-sou, Lett. Nuovo Cimento **37**, 495 (1983); Cai Xu, Liu Lian-sou, and Meng Ta-chung, Comm. Theor. Phys. (to be published).

[11]W. Thome *et al.*, Nucl. Phys. **B129**, 365 (1977).

[12]UA5 Collaboration, G. J. Alner *et al.*, Phys. Lett. **138B**, 304 (1984).

[13]UA1 Collaboration, G. Arnison *et al.*, Phys. Lett. **123B**, 108 (1983).

[14]Cai Xu, Liu Lian-sou, and Meng Ta-chung, Phys. Rev. D **29**, 869 (1984).

[15]Liu Lian-sou, Qin Li-hong, and Zhuang Peng-fei, Hua-Zhong Normal University Report No. HZPP 85-1 (unpublished).

[16]T. T. Chou and C. N. Yang, Phys. Lett. **B135**, 175 (1984).

[17]See, for example, the following: P. Aurenche and F. W. Bopp, Z. Phys. C **13**, 205 (1982); S. Barshay, Phys. Lett. 116B, 193 (1982); A. Capella and J. Tran Thanh Van, *ibid.* **114**, 450 (1982); Z. Phys. C **18**, 85 (1983); **23**, 165 (1984); A. B. Kaidalov and K. A. Ter-Martirosyan, Phys. Lett. **117B**, 249 (1982); C. S. Lam and P. S. Yeung, *ibid.* **119B**, 445 (1982); Y. K. Lim and K. J. Phua, Phys. Rev. D **26**, 785 (1982); F. Takagi, Z. Phys. C **13**, 301 (1982); **19**, 213 (1983); P. Carruthers and C. C. Shih, Phys. Lett. **127B**, 242 (1983); G. Pancheri and Y. N. Srivastava, *ibid.* **128B**, 433 (1983); P. Aurenche, F. W. Bopp, and J. Ranft, Z. Phys. C **23**, 67 (1984); M. Biyajima, Phys. Lett. **137B**, 225 (1984); **139B**, 93 (1984); M. Blazek, University of Bratislava report (unpublished); G. Pancheri and C. Rubbia, Nucl. Phys. **A418**, 117c (1984); A. Bialas, I. Derado, and L. Stodolsky, Phys. Lett. **156B**, 421 (1985); G. Pancheri, Y. Srivastava, and M. Pallotta, *ibid.* **151B**, 453 (1985); D. C. Hinz and C. S. Lam, McGill University report, 1985 (unpublished), and references given therein.